



## **THE ROLE OF TEMPERATURE GRADIENTS IN API N80 PIPE CORROSION**

**BOUZID NOUREDDINE<sup>\*</sup>, BEBBA AHMED ABDELHAFID<sup>a</sup>,  
SETTOU NOUREDDINE<sup>a</sup> and DJELLOUL ABDELKADER<sup>b</sup>**

Laboratoire de Physique des Matériaux, Université de Ouargla, BP 511, 30000 Ouargla, ALGÉRIE

<sup>a</sup>Laboratoire de Valorisation et de Promotion des Ressources Sahariennes, BP 511,  
30000 Ouargla, ALGÉRIE

<sup>b</sup>ASPIA Laboratoire des Structures, Propriétés et Interactions Inter Atomiques, Centre Universitaire de  
Khenchela, 40000 Khenchela, ALGÉRIE

### **ABSTARCT**

This paper presents some investigations on the effect of temperature gradient in API N80 pipe corrosion. It was possible to highlight the existence of temperature gradient on the walls of pipe, variable along the depth of producing water Albian wells and reaches 16°C. The chemical analyses of the water samples of several drillings show that these last are of petrifying nature, charged with sulfates, low content of dissolved carbon dioxide and no oxygen. The XRD analyses of the scale show that it is heterogeneous and primarily consists of siderite (FeCO<sub>3</sub>), goethite (FeOOH), hematite (Fe<sub>2</sub>O<sub>3</sub>), magnetite (Fe<sub>3</sub>O<sub>4</sub>) and of calcite (CaCO<sub>3</sub>). The perforation of the pipes was mainly due to the detached matter with the variations in temperatures along the wells.

**Key words:** API N80 pipe, Albian water, Corrosion, Termometry, Temperature gradient.

### **INTRODUCTION**

The area of Haoud-Berkaoui, subject of this study, includes three producing crude oil fields, Haoud-Berkaoui, Benkahla and Guellala. It is located about 100 km west of Hassi-Messaoud (Algeria). The oil extraction from this heterogeneous layer of average size is assisted by the pressure injection of Albian water in the geological formations. The Albian is a fossil and deep aquifer (2000 meters in depth) extending on a surface of 60000 Km<sup>2</sup> and covers all Algerian south-east. Its capacity is estimated to be 50000 billion m<sup>3</sup>; it contains no oxygen. Owing to the development of the drilling techniques, the exploitation of this aquifer extended to the oil field, in particular in the operations of keeping well pressure by water injection. Water is extracted from 15 well (producing wells) feeding an

---

<sup>\*</sup> Author for correspondence; Email: bz\_djamel5@yahoo.fr; Tel.: +213 775590814; Fax: +21329712627

injection unit made up of high pressure several electropumps provided with sand filters with a smoothness of  $2\mu$ .

Filtered water is then sent to the injecting wells (32 wells) to maintain the pressure of the layer. The fixture of pressure holding by water injection involves wells sources (producing water wells), a pumping unit and a chemical treatment unit designed in such a way that it allows the injection of the corrosion inhibitors in the steel pipes. These concentric pipes have an internal diameter of 4.216 cm and are laid out co-axially and end to end by threading along the tubes of production (Fig.1).

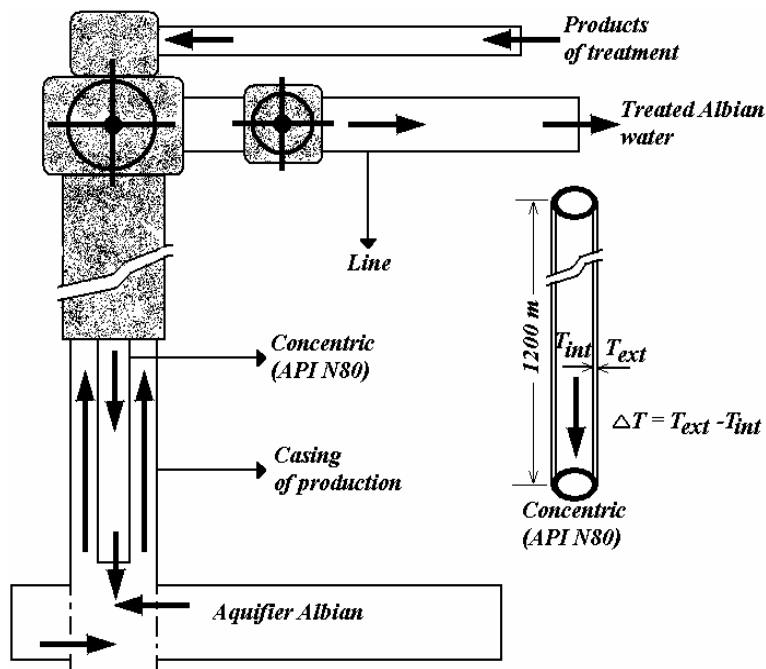


**Fig. 1: Synoptic schema of a producing water well**

The wells sources are drilled to a depth of 1000 to 1300 m with a completion composed of production tubes (casing) having a diameter of 17.78 cm, an overall length of 1123 m, and of a treatment trimming. The surface equipment and basic parts of the injection system must be protected from the corrosion, which can cause the boring of the casings. The lifetime of the pipes, planned initially for five years, was strongly reduced to only two years. The concentric pipes were in a very advanced state of corrosion with apparent borings. The waste in time and money due to the replacement operations was considerable, the estimated is approximately 300 000 US dollars per year.

The corrosion of the pipes is due to several factors such as the quality of water, its composition, the flow conditions and the inhibitors.

Corrosion is an electrochemical process. It is a time dependent mechanism and depends on the local environment within or adjacent to the pipeline. Corrosion usually appears as either general corrosion or localised (pitting) corrosion. It can occur on the internal or external surfaces of the pipe, and in the base material.

Corrosion of the iron pipe is influenced by many different factors including water quality, composition, and flow conditions. According to AWWARF and DVGW<sup>1</sup>, the indices of Langelier and Ryznard do not reflect the real state of corrosion. McNeill and Edwards<sup>2</sup> found that changes in water quality parameters, pH and alkalinity, could not fully account for observed changes in corrosion of iron pipes under stagnant conditions and thus, water quality cannot always explain variation in corrosion behaviour.

The temperature is an important factor in the corrosion process. It affects the rate of corrosion and the solubility of solids. It is necessary to consider two aspects in connection with this parameter. The first is due to the fact that corrosion can be significantly different from a constant temperature to another and this is for the same quality of water, while the second is related to the fact that the pipes subjected to a variation in temperature (increasing, decreasing or cyclic) over shorter periods corrode differently from those, which remain at constant temperatures.

A recent review suggests that serious mechanical stresses could arise within pipes due to temperature changes, mainly because the protective scale on pipes has a different coefficient of thermal expansion than the metal itself<sup>3</sup>. Rezanian and Anderi<sup>4</sup> consider that such changes in temperature might be responsible for the high release of copper to water observed in some cases during winter months. Rushing and Edwards<sup>5</sup> confirmed and explored this effect further and reported that these problems might also be caused by sustained temperature gradients applied to residential copper pipes. Temperature changes had been suspected to increase copper pitting frequency and copper release to drinking water. Experiments examined the effect of temperature gradients on copper pipe corrosion during stagnant conditions. The pipe orientation in relation to the temperature gradient determined whether convective mixing would occur, which influenced temperature gradients within the pipe. This work showed that temperature gradients of 20°C lead to thermogalvanic currents, which influences copper leaching and scale type.

The present study aims to determine profile of temperature along the pipe using the

digital simulation of the flow by thermometry and to examine the effect of this factor on rapid degradation of concentric pipes in Albanian water.

## EXPERIMENTAL

### Numerical Simulations of the Flow and Experimental Methods

#### Thermometry

The knowledge of the temperature profiles under the static and dynamic conditions of the producing water wells and the evolution of this profile according to the produced water flow is necessary to evaluate the working procedure of the well. We wish to determine in counter-current flow mode, the evolution of the variation in temperature  $\Delta T$  on the walls of treatment concentric pipes along a producing water well ( $\Delta T = T_{\text{ext}} - T_{\text{int}}$ ). We are interested in the modeling of the incompressible and viscous flows in axisymmetric and annular pipes. These flows can be laminar or turbulent with important longitudinal variations in temperature in various geometrical configurations involving many phenomena. Among these phenomena, the important variation of the temperature can affect the nature of the flow in the study field<sup>6</sup>. The selected model thus requires the writing of an equation governing the temperature rising from the principle of energy conservation of convection diffusion type<sup>7</sup>.

The modeling of the flows is described by mathematical relations between the rates of flow (U, V), the pressure P and the temperature T in a cylindrical coordinates (O, r, z). This was possible because of the use of the balance equations deduced from the principles of conservation of the mass, the momentum and the energy, which are –

Continuity Equation:

$$\frac{1}{r} \frac{\partial}{\partial r} (rV) + \frac{\partial U}{\partial z} = 0 \quad \dots (1)$$

Momentum equation on Oz axis:

$$\begin{aligned} \rho \left( V \frac{\partial U}{\partial r} + U \frac{\partial U}{\partial z} \right) = & - \left( \frac{1}{Fr^2} \right) \rho - \frac{\partial P}{\partial z} + \left( \frac{1}{Re} \right) \mu \left( \frac{\partial^2 U}{\partial z^2} + \frac{1}{r} \frac{\partial}{\partial r} \left( r \frac{\partial U}{\partial r} \right) \right) \quad \dots (2) \\ & + \left( \frac{1}{Re} \right) \frac{d\mu}{dT} \left( 2 \frac{\partial T}{\partial z} \cdot \frac{\partial U}{\partial z} + \frac{\partial T}{\partial r} \left( \frac{\partial V}{\partial z} + \frac{\partial U}{\partial r} \right) \right) \end{aligned}$$

Momentum equation on Or axis:

$$\rho \left( V \frac{\partial V}{\partial r} + U \frac{\partial V}{\partial z} \right) = -\frac{\partial P}{\partial r} + \left( \frac{1}{\text{Re}} \right) \mu \left( \frac{\partial^2 V}{\partial z^2} + \frac{1}{r} \frac{\partial}{\partial r} \left( r \frac{\partial V}{\partial r} \right) - \frac{V}{r^2} \right) + \left( \frac{1}{\text{Re}} \right) \frac{d\mu}{dT} \left( 2 \frac{\partial T}{\partial r} \cdot \frac{\partial V}{\partial r} + \frac{\partial T}{\partial z} \left( \frac{\partial V}{\partial z} + \frac{\partial U}{\partial r} \right) \right) \quad \dots (3)$$

Energy equation:

$$\rho \left( V \frac{\partial T}{\partial r} + U \frac{\partial T}{\partial z} \right) = \left( \frac{1}{\text{Re Pr}} \right) \left[ \frac{1}{r} \frac{\partial}{\partial r} \left( r \frac{\partial T}{\partial r} \right) + \frac{\partial^2 T}{\partial z^2} \right] + 2\mu \left( \frac{1}{\text{Re Ec}} \right) \left[ \left( \frac{\partial V}{\partial r} \right)^2 + \left( \frac{V}{r} \right)^2 + \left( \frac{\partial U}{\partial z} \right)^2 \right] + \mu \left( \frac{1}{\text{Re Ec}} \right) \left( \frac{\partial V}{\partial z} + \frac{\partial U}{\partial r} \right)^2 \quad \dots (4)$$

In these equations, Fr, Re, Pr, EC are Froude, Reynolds, Prandtl and Eckert numbers.  $\mu$  and  $\rho$  are dynamic viscosity and fluid density, respectively.  $\mu$  is expressed in  $\text{Kg.m}^{-1}.\text{s}^{-1}$  by the relationship:  $\mu = \frac{\mu_0}{1 + aT + bT^2}$ , where  $\mu_0 = 1.161 \cdot 10^{-3} \text{ Kg.m}^{-1}.\text{s}^{-1}$ ,  $a = 0.033368^\circ\text{C}^{-1}$ ,  $b = 0.00022^\circ\text{C}^{-2}$  (Joulie, 1998)<sup>8</sup> and  $\rho = 998.8 \text{ Kg.m}^{-3}$ . The model chosen for turbulence is the model of mixture length (model zero equation). It presents a good approach for the taking into account of the turbulent effects in cylindrical pipes<sup>9</sup>. These equations are discretized by the finite-volume method (FVM) using two types of grids; a grid shifted to evaluate the field speed, and a principal grid centered to evaluate the pressure and the temperature. The SIMPLE algorithm (Semi-Implicit Method for Pressures-Linked Equation) was used for the resolution of discrete equations<sup>10</sup>.

The linear system is then solved by the algorithm TDMA (TriDiagonal-Matrix Algorithm) which consists of carrying out a screening of the field of calculation line by line or column by column; this algorithm is translated into a data-processing program written in FORTRAN.

## Water analysis

The water samples were taken at the head of producing water wells. Eight drillings

of the area of Haoud Berkaoui were selected for this purpose. The samples were done in polyethylene bottles after a few hours of well discharging. All the taking away operations were carried out according to the methods of Rodier<sup>11</sup> and standards AFNOR<sup>12</sup>. The principal analyzed chemical factors were the pH, calcium, magnesium, potassium, sodium, chlorides, bicarbonates, sulfates, nitrates and dissolved carbon dioxide.

### **X-ray diffraction**

The X-ray experiments were carried out on corrosion scales taken at various depths of concentric pipes after two years of well exploitation. Samples were identified and characterized by X-ray diffraction analysis using Philips model PW1700, the tension, intensity and the scanning rate are 34 kV, 22 mA and 2 °/mn, respectively.

## **RESULTS AND DISCUSSION**

The profile of temperature was given after evaluation of the flow conditions characterized by Reynolds and Prandtl numbers for the two fluids taking into account that the inhibitor injection was done continuously, with the inlet temperature of 25 °C and with a concentration of 20 ppm equivalent to a flow of 0.1 m<sup>3</sup>/h. The hot fluid (Albian water), flows in the annular space from the bottom up to the surface with a flow of 23.5 m<sup>3</sup>/h (corresponding to the real value of the flow of producing wells which varies from 23.5 m<sup>3</sup>/h to 57 m<sup>3</sup>/h) and an inlet temperature of 60 °C (corresponding to the real wellbottom temperature). The results of calculations are shown in Fig. 2, which indicates that the variation in temperature gradient is relatively low at the wellhead, and then increases considerably when the depth reached 584 m. For a depth ranging between 584 m and 984 m,  $\Delta T$  somewhat increases and remains however high. It is in this zone, where the API N80 pipe is most affected by corrosion ( $\Delta T$  can reach 16°C).

Visual examination of concentric taken from well GLAHA2 after two years exploitation revealed corrosion on the external surface. The pipe was covered with brownish deposit of 2 mm thick; its distribution is heterogeneous and with apparent pinholes of diameter varies from 5 to 10 mm (Fig.3).

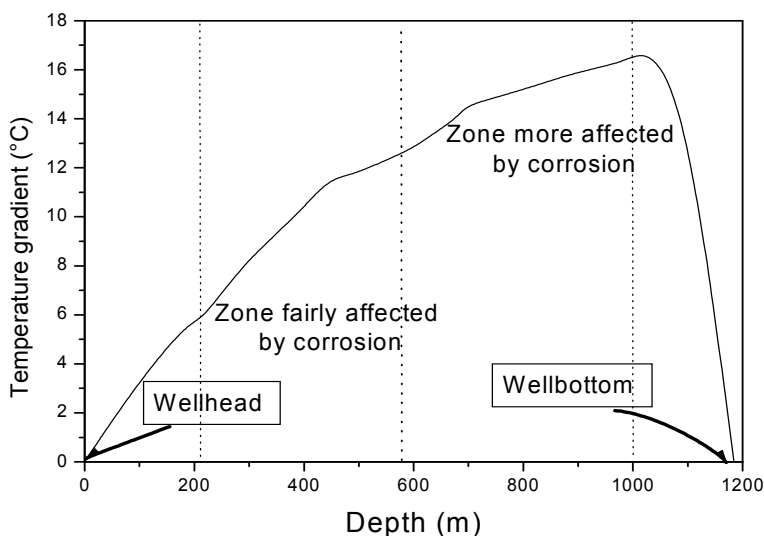


**Fig. 2: Temperature gradient as a function of well depth GLAHA2**

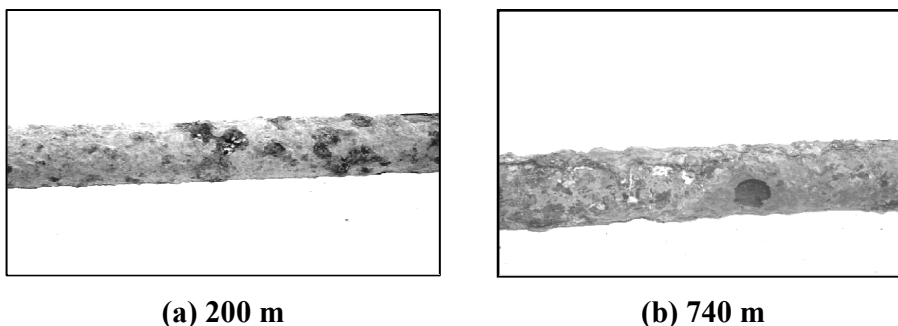


**Fig. 3: General aspect of pipes after two years exploitation period**

The results of the chemical analyses and those of the marble tests are presented in Table 1. From a drilling to another, the ions contents vary from 107 to 258 mg.L<sup>-1</sup> for calcium, from 73 to 139 mg L<sup>-1</sup> for magnesium, from 24 to 36 mg L<sup>-1</sup> for potassium, from 282 to 304 mgL<sup>-1</sup> for sodium, from 459 to 648 mg L<sup>-1</sup> for chlorides and from 116 to 176 mg L<sup>-1</sup> for bicarbonates. The obtained values show that the chemical compositions of the various drillings are relatively identical and the observed disparities are not very significant. In general it is earthy water, chlorinated and rich in sulfates, but almost

deprived of dissolved gas. The quantities of dissolved  $\text{CO}_2$  are relatively low and mostly in the form of  $\text{HCO}_3^-$ . The alkalinity of this water is entirely due to bicarbonates. The pH is neutral or slightly basic and hence, favors the formation of tartar ( $\text{CaCO}_3$ ). All the saturation indices are positive thus, the water is of petrifying nature. Moreover, water quality can not always explain variation in corrosion behavior<sup>2</sup>.

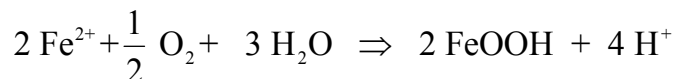
**Table 1. Chemical analyses and marble tests for the waters of Haoud-Berkaoui area**

Wells	GLAHA1	GLAHA2	OKJHA3	GLAHA4	OKJHA4	OKJ21	OKM88
$\text{Ca}^{2+}$ (mg.L <sup>-1</sup> )	194	181	258	171	154	139	132
$\text{Mg}^{2+}$ (mg.L <sup>-1</sup> )	78	75	86	121	139	114	33
$\text{K}^+$ (mg.L <sup>-1</sup> )	32	32	32	31	35	36	33
$\text{Na}^+$ (mg.L <sup>-1</sup> )	282	298	304	294	285	282	245
$\text{Cl}^-$ (mg.L <sup>-1</sup> )	470	459	472	481	648	562	596
$\text{HCO}_3^-$ (mg.L <sup>-1</sup> )	176	170	161	131	137	137	139
$\text{SO}_4^{2-}$ (mg.L <sup>-1</sup> )	546	618	762	564	523	450	465
$\text{NO}_3^-$ (mg.L <sup>-1</sup> )	13	10	13	14	10	12	11
$\text{CO}_2$ (mg.L <sup>-1</sup> )	18	18	22	28	35	37	16
pH	7.47	7.02	7.58	7.14	7.20	7.20	7.26
pHs	6.87	6.88	6.83	6.86	6.72	6.58	6.70
Is	0.60	0.14	0.75	0.28	0.48	0.62	0.56

The X-ray diffraction patterns shown in the Fig. 4a, 4b, 4c and 4d indicate that the scale is made up of siderite ( $\text{FeCO}_3$ ), goethite ( $\text{FeOOH}$ ), hematite ( $\text{Fe}_2\text{O}_3$ ), magnetite ( $\text{Fe}_3\text{O}_4$ ), calcite ( $\text{CaCO}_3$ ), barite ( $\text{BaSO}_4$ ) and silica ( $\text{SiO}_2$ ). The presence of silica is inevitable and it comes primarily from the sand involved with water throughout the period

of exploitation while barite is resulting from the mud used in the operation of snubbing.

We propose the following mechanism to explain the experimental results:



Oxygen is introduced into the wells during inhibitors injection operation and  $\text{Fe}^{2+}$  ions come from iron dissolution,

The formed goethite acts with  $\text{Fe}^{2+}$  ions, in the same way as with oxygen, as an oxidizer and give the magnetite,



Magnetite gives hematite by oxidation reaction,



A pilot pipe distribution study conducted over one year under various blended waters (i.e. blends of ground, surface and saline waters) had shown that iron release from aged pipes varied with blended qualities as well as aged pipe materials. Based on XRD and RMS results,  $\text{FeCO}_3$ ,  $\alpha\text{-FeOOH}$ ,  $\beta\text{-FeOOH}$ ,  $\gamma\text{-Fe}_2\text{O}_3$  and  $\text{Fe}_3\text{O}_4$  were identified as primary corrosion products of unlined cast iron pipes, No significant  $\text{FeCO}_3$  was detected by XPS analysis in corrosion scales. This is because  $\text{FeCO}_3$  is very unstable and would transform in  $\text{Fe}_2\text{O}_3$  on contact with air<sup>13</sup>.

For API N80 pipes and Albian water quality, the formation of one or the other of the various products of corrosion depends strongly on temperature, which affects solution properties (such as viscosity) and thermodynamic properties (such as activity coefficient, enthalpy of reaction and solubility).

On one hand, the increase of temperature involves a decrease in the viscosity of water. This will allow increased transport of reactants and products ( $\text{Fe}^{+2}$  species) to and from the metal surface due to increased diffusion, involving an increase of the corrosion rate<sup>14, 15</sup>.

On the other hand, the activity coefficients of specific ions present in waters changes with temperature. According to McNeill and Edwards<sup>2</sup>, the activity coefficients increases slightly, when the temperature passed from 25°C to 5°C and at the same time, the

solubility of a solid phase increase or decrease according to the sign of the enthalpy of reaction.

Stumm and Morgan and Pankow studies showed a 0.32 and 0.77 log change in product solubility of FeOOH and FeCO<sub>3</sub>, respectively. All these changes lead to the formation of a product rather than another leading to a heterogeneous deposit. This heterogeneity makes the iron scale susceptible to two physical exchanges as the temperature varies i.e. different density and different coefficient of thermal expansion.

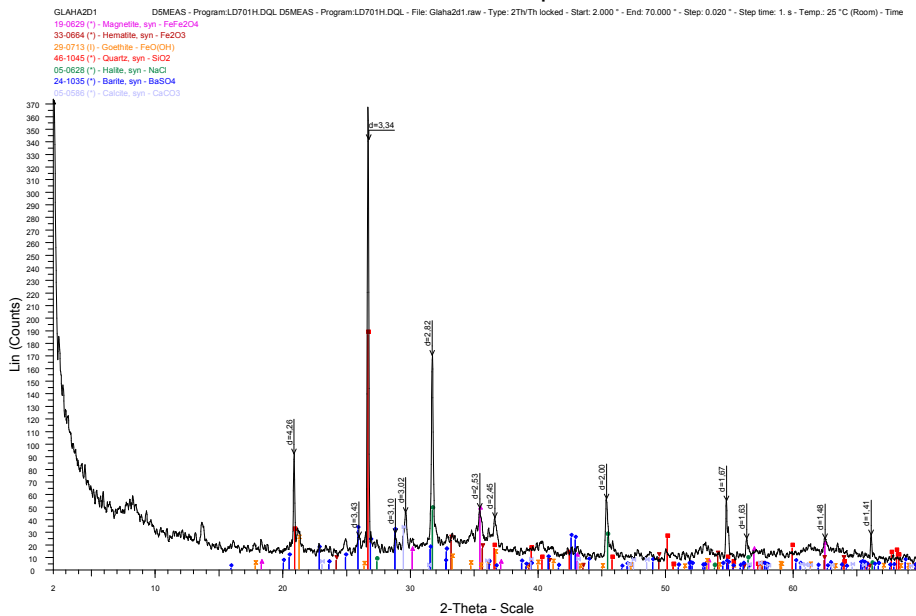
Because the scale is heterogeneous, i.e. different scale components have different densities; thus, any PBR  $\neq$  1 (Pilling-Bedworth Ratio) indicates that compressive or tensile stresses may be introduced into the scale, depending on the surface geometry (generally greater for concave or convex surfaces). This aspect is important, when a new type of scale forms as the temperature is varied.

**Table 2. Pilling-Bedworth ratios (PBR) values**

Compounds	PBR	Compounds	PBR
Fe <sub>2</sub> O <sub>3</sub> : Fe	2.143	FeOOH : Fe <sub>2</sub> O <sub>3</sub>	1.371
Fe <sub>3</sub> O <sub>4</sub> : Fe	2.103	FeOOH : Fe <sub>3</sub> O <sub>4</sub>	1.397
FeOOH : Fe	2.939	Fe <sub>2</sub> O <sub>3</sub> : Fe <sub>3</sub> O <sub>4</sub>	1.018

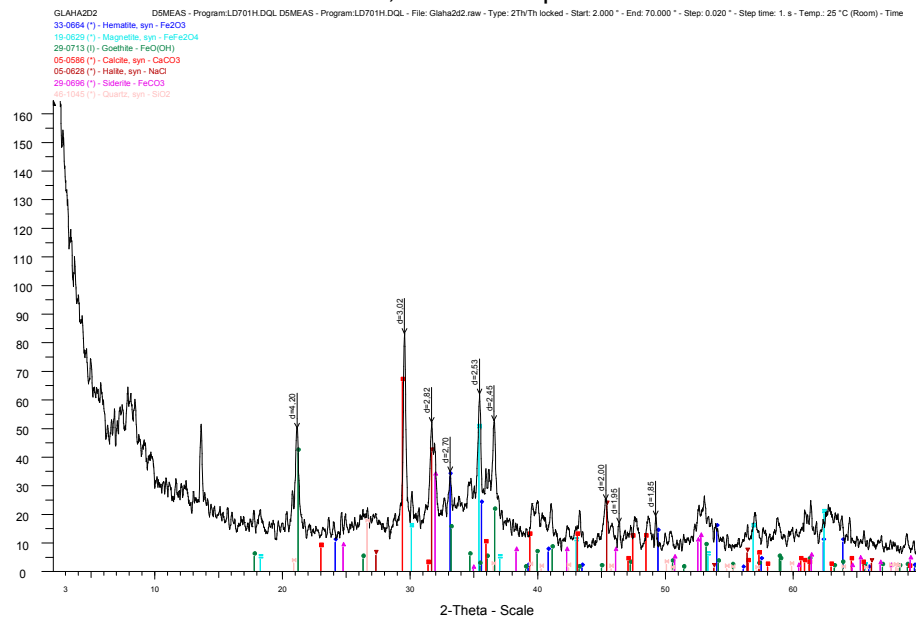
By elsewhere, a particular scale component will have a different coefficient of thermal expansion ( $\alpha$ ) compared to the metal or other layers of scale. Fe metal ( $\alpha = 15.30 \times 10^{-6} \text{ }^\circ\text{C}^{-1}$ ) will expand and contract nearly 46% more than Fe<sub>3</sub>O<sub>4</sub> scale ( $\alpha = 10.50 \times 10^{-6} \text{ }^\circ\text{C}^{-1}$ ) and 40% more than Fe<sub>2</sub>O<sub>3</sub> scale ( $\alpha = 10.96 \times 10^{-6} \text{ }^\circ\text{C}^{-1}$ ) in response to the same temperature change. These differences cause mechanical stresses also in the scale as the temperature changes and become more important with decreasing diameter pipes (the case of the API N80 pipe); the stresses can lead to scale spalling or crack formation<sup>18</sup>. In a study of cast iron studs placed in distribution system pipes, an increase in iron concentration in the water was observed when deep cracks appeared in the scale on the iron studs<sup>19</sup>. Such phenomena might expose unprotected metal surface to the solution; thus, drastically increasing corrosion rates and, as a consequence, the reduction of pipeline lifetime.

### Echantillon 1, Glaha-2 prof.=0 m



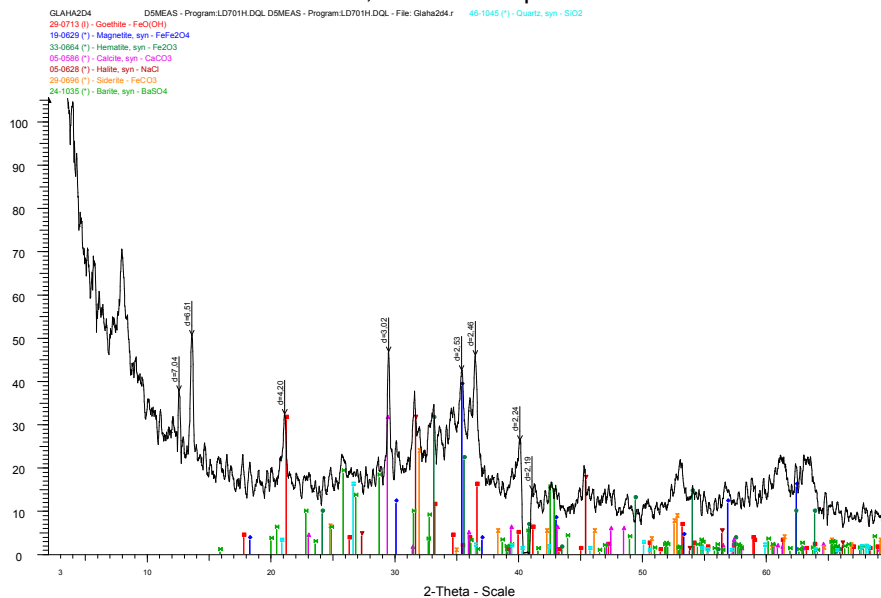
(a): 0 m

### Echantillon 2, GLAHA-2 prof.= 200 m



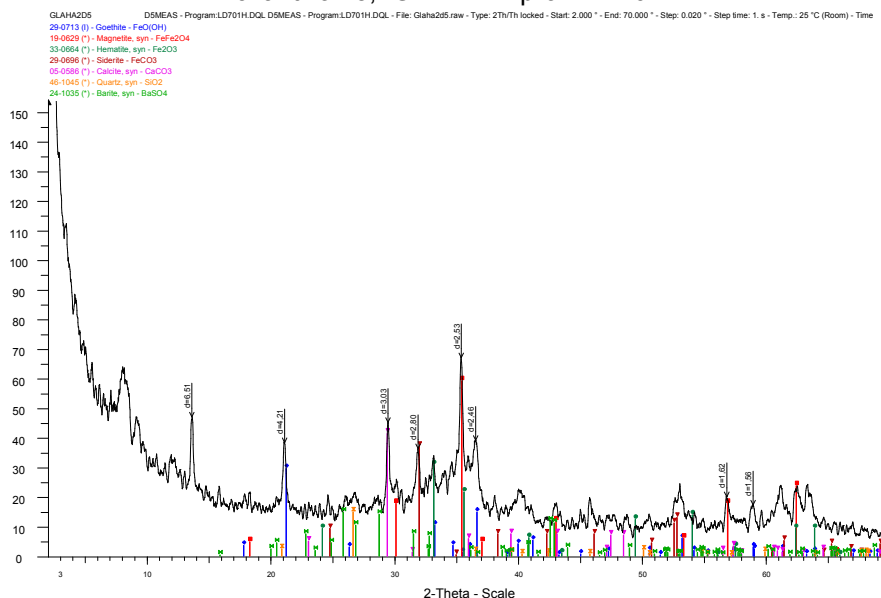
(b) 200 m

## Echantillon 4, GLAHA-2 prof. = 570 m



(c) 570 m

## Echantillon 5, GLAHA-2 prof. = 740 m



(d) 740 m

Fig. 4: XRD patterns of corrosion scale formed at different depths

## CONCLUSION

The results of the chemical analyses of the water of the various wells and the values of the indices of saturation show that the water of the Albian aquifer of Haoud-Berkaoui is of furring nature. It is not very charged of dissolved gas, its alkalinity is entirely due to bicarbonates and the pH of various drillings is neutral or slightly basic.

The simulation of the flows showed the existence of a temperature gradient, variable with depth and reached 16 °C. The concentric pipes taken from the well after two years working period were in a very advanced state of degradation presenting perforations corresponding to the highest temperature gradient. The analyses of the corrosion scale show that they are heterogeneous. The formation of one or another of the products of corrosion is closely related to the variation in temperature which affects the physical properties of the deposited compounds. This involves detachments of matters and appearance of pinholes and consequently, the lifetime of the pipes decreases.

## ACKNOWLEDGEMENTS

This work was supported by Algerian company of oil (Sonatrach, No I/133/HMD/2000). The authors wish to thank them for the permission to publish this work. This paper would not have been possible without the assistance of many members of the Development and Research Centre of Boumerdes staff.

## REFERENCES

1. American Water Works Association Research Foundation and DVGW-Technologiezentrum Wasser, Internal Corrosion of Water Distribution Systems, American Water Works Association, Denver, CO, (1996).
2. L. S. McNeill and M. Edwards, Iron Pipe Corrosion in Drinking Water Distribution Systems, *J. AWWA* **93(7)**, 88–100 (2001).
3. L. S. McNeill and M. Edwards, The Importance of Temperature in Assessing Iron Pipe Corrosion in Water Distribution Systems, *Environmental Monitoring and Assessment* **77(3)**, 229–242 (2002).
4. L. Rezania and W. Anderi, Copper Corrosion and Iron Removal Plants, The Minnesota Experience. AWWA WQTC, New Orleans, LA, (1995).
5. J. C. Rushing and M. Edwards, The Role of Temperature Gradients in Residential Copper Corrosion, *Corrosion Science*, **46(8)**, 1883-1894 (2004).

6. M. A. Dos Bernardes, Numerical Analysis of Natural Laminar Convection in Radial Solar Heater, *International J. Thermal Sci.*, **38**, 42-50 (1999).
7. R. Comolet, *Experimental Fluid Mechanics*, Vol. 2, Fourth Edition, Masson, Paris.
8. R. Joulie, (1998). *Mécanique des fluides appliqués*, ELLIPSES, Paris (1994).
9. L. Bencharif, Calcul d'un écoulement méridien en fluide parfait ou visqueux par une méthode basée sur la dynamique du rotationnel. D. Sc. Thesis. Paris VI University. Notes et documents LIMSI 93-94 (1993).
10. S. V. Patankar, *Numerical Heat Transfer and Fluid Flow*, Hemisphere Publishing Corporation, USA (1980).
11. J. Rodier, *Water Analysis*, 8th Edition; DUNOD, Paris (1996).
12. AFNOR, Collection of the French Standardization Association, *Water Test Methods* (1990).
13. Z. Tang, S. Hong, W. Xiao and J. Taylor, Characteristics of Iron Corrosion Scales Established under Blending of Ground, Surface and Saline Waters and their Impacts on Iron Release in the Pipe Distribution System, *Corrosion Science*, **48(2)**, 322-342 (2006).
14. J. Davalos, M. Gracia, J. F. Marco and J. R. Gancedo, Corrosion of Weathering Steel and Iron under Wet-dry Cycling Conditions, Influence of the Rise of Temperature During the Dry Period, *Hyperfine Interactions*, **69(1-4)**, 871-874 (1991).
15. K. Mabuchi, Y. Horii, H. Takahashi and M. Nagayama, Effect of Temperature and Dissolved Oxygen on the Corrosion Behaviour of Carbon Steel in High-Temperature Water, *Corrosion*, **47(7)**, 500-508 (1991).
16. W. Stumm and J. J. Morgan, *Aquatic Chemistry, Chemical Equilibria and Rates in Natural Waters*, John Wiley & Sons, Inc. New York, NY (1996).
17. J. F. Pankow, *Aquatic Chemistry Concepts*, Lewis Publishers, Chelsea, MI (1991).
18. M. Schutze, *Protective Oxide Scales and their Breakdown*, John Wiley & Sons, West Sussex, England (1997).
19. S. E. Smith, T. Ta, D. M. Holt, A. Delanoue and J. S. Colbourne, Minimising Red Water in Drinking Water Distribution Systems, in *Proceedings of AWWA Water Quality Technology Conference*, San Diego, CA, American Water Works Association, Paper 5 C-5 (1998).